HHS Public Access

Author manuscript

Mol Pharm. Author manuscript; available in PMC 2023 January 05.

Published in final edited form as:

Mol Pharm. 2023 January 02; 20(1): 500–507. doi:10.1021/acs.molpharmaceut.2c00744.

Inactivated Cowpea Mosaic Virus for In Situ Vaccination: Differential Efficacy of Formalin vs UV-Inactivated Formulations

Eunkyeong Jung◆,
Department of Nanoengineering, University of California San Diego, La Jolla, California, 92093, United States

Chenkai Mao◆,
Department of Microbiology and, Immunology, Dartmouth Geisel School of Medicine, Hanover, New Hampshire 03755, United States

Misha Bhatia,
Department of Nanoengineering, University of, California San Diego, La Jolla, California 92093, United, States

Edward C. Koellhoffer,
Radiology, University of California San Diego, La Jolla, California 92093, United States

Steven N. Fiering,
Department of Microbiology and, Immunology and Dartmouth Cancer Center, Dartmouth, Geisel School of Medicine, Hanover, New Hampshire 03755, United States

Nicole F. Steinmetz
Department of Nanoengineering, Radiology, Bioengineering, Moores Cancer Center, Center for Nano-Immuno Engineering, and Institute for Materials, Design and Discovery, University of California San Diego, La, Jolla, California 92093, United States

Abstract

Cowpea mosaic virus (CPMV) has been developed as a promising nanoplatform technology for cancer immunotherapy; when applied as in situ vaccine, CPMV exhibits potent, systemic, and durable efficacy. While CPMV is not infectious to mammals, it is infectious to legumes; therefore, agronomic safety needs to be addressed to broaden the translational application of CPMV. RNA-containing formulations are preferred over RNA-free virus-like particles because the RNA and protein, each, contribute to CPMV's potent antitumor efficacy. We have previously optimized inactivation methods to develop CPMV that contains RNA but is not infectious to plants. We established that inactivated CPMV has reduced efficacy compared to untreated, native CPMV. However, a systematic comparison between native CPMV and different inactivated forms of

Corresponding Author: Nicole F. Steinmetz nsteinmetz@ucsd.edu.
◆**Author Contributions:** E.J. and C.M. contributed equally.

Complete contact information is available at: https://pubs.acs.org/10.1021/acs.molpharmaceut.2c00744

The authors declare the following competing financial interest(s): Drs. Fiering and Steinmetz are co-founders of and have a financial relationship with Mosaic Immunoengineering Inc, which may be considered potential competing interest. Dr. Steinmetz serves as Acting Chief Scientific Officer, Board Member, and paid Consultant to Mosaic; Dr. Fiering serves as paid Consultant to Mosaic. The other authors declare no other potential conflict of interest.

CPMV was not done. Therefore, in this study, we directly compared the therapeutic efficacies and mechanisms of immune activation of CPMV, ultraviolet- (UV-), and formalin (Form)-inactivated CPMV to explain the differential efficacies. In a B16F10 melanoma mouse tumor model, Form-CPMV suppressed the tumor growth with prolonged survival (there were no statistical differences comparing CPMV and Form-CPMV). In comparison, UV-CPMV inhibited tumor growth significantly but not as well as Form-CPMV or CPMV. The reduced therapeutic efficacy of UV-CPMV is explained by the degree of cross-linking and aggregated state of the RNA, which renders it inaccessible for sensing by Toll-like receptor (TLR) 7/8 to activate immune responses. The mechanistic studies showed that the highly aggregated state of UV-CPMV inhibited TLR7 signaling more so than for the Form-CPMV formulation, reducing the secretion of interleukin-6 (IL-6) and interferon-α (IFN-α), cytokines associated with TLR7 signaling. These findings support the translational development of Form-CPMV as a noninfectious immunotherapeutic agent.

Graphical Abstract

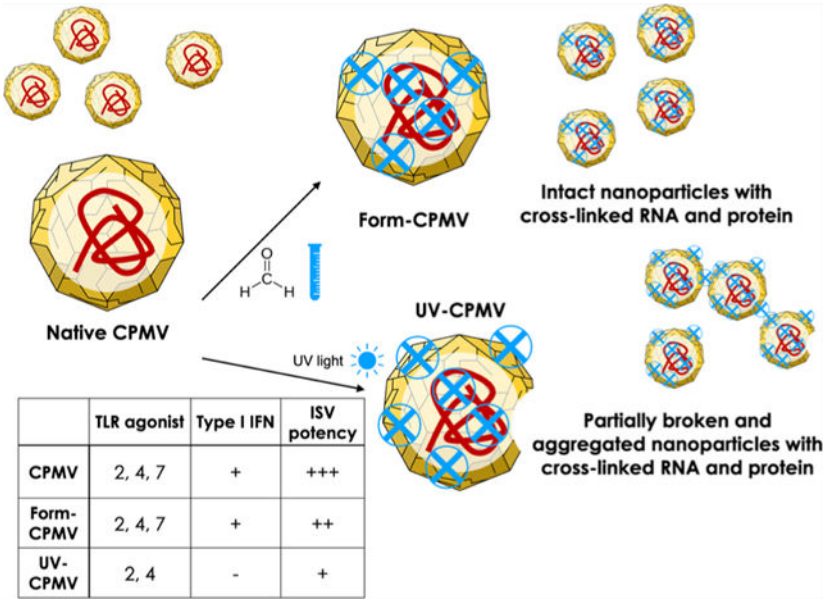

	TLR agonist	Type I IFN	ISV potency
CPMV	2, 4, 7	+	+++
Form-CPMV	2, 4, 7	+	++
UV-CPMV	2, 4	-	+

Keywords

cowpea mosaic virus; in situ vaccine; cancer immunotherapy; inactivation; formalin; UV light

INTRODUCTION

Advances in cancer immunotherapy have demonstrated that the modulation of the patient's immune system can generate a dramatic antitumor activity. One approach is termed in situ vaccination (ISV): here, an immune stimulatory agent is administered directly into an injectable tumor to remodel the immunosuppressive tumor microenvironment (TME). While the agent typically acts on innate immune cells, the ultimate goal is to launch systemic antitumor immunity with effector T cells responding against the patient's tumor-associated

and neoantigens to protect against metastasis or recurrence. Many ISV approaches are undergoing pre- and clinical developments; these include Toll-like receptor (TLR) agonists and stimulator of interferon (IFN) genes STING agonists, delivered by either injection of soluble small-molecule agonist or packaged into nanoparticles.[1] For example, the intratumoral injection of CMP-001, a TLR9 agonist under clinical trial, showed efficacy in combination with anti-PD-1 in advanced melanoma (clinical trial: NCT04698187). Oncolytic viruses have also been engineered to function as in situ vaccines. For example, Amgen's Imlygic is based on an attenuated herpes simplex virus engineered to express the cytokine granulocyte-macrophage colony-stimulating factor (GM-CSF)—intratumoral administration results in tumor cell killing mediated by the oncolytic function of the virus and recruitment and activation of innate immune cells to process tumor-associated antigens (TAAs) and neoantigens released from the tumor cells to prime systemic antitumor immunity.[2]

As a noninfectious viral option (i.e., noninfectious toward mammals), plant viruses have value as next-generation ISV approaches. A number of plant viruses have been investigated as in situ vaccines with differential potency.[3] One group reported the potency of virus-like particles of the papaya mosaic virus (PapMV) that activates the innate immune response in an IFN-α-dependent manner. It has shown efficacy in synergy with dendritic cell (DC)-based vaccination and PD-1 blockade by potentiating antitumor immune responses.[4] Our labs discovered that cowpea mosaic virus (CPMV) induces potent, systemic, and durable antitumor immunity when used as in situ vaccine, with efficacy demonstrated in multiple tumor mouse models[5,6] as well as companion canine patients.[7] Although CPMV is noninfectious toward mammals, it is potently immunogenic. The nucleoprotein assembly is not enveloped and stimulates TLRs 2, 4, and 7 that recognize and respond to pathogen-associated molecular patterns (PAMPs).[8] The multivalency of the capsid and multiple TLR activation improves efficacy vs single TLR or STING agonists.[5,6] Mechanistically, the in situ vaccination of CPMV (CPMV-ISV) modulates the TME by activating the innate immune cells (switch of M2 to M1 macrophages, recruitment and activation of natural killer (NK) cells, dendritic cells (DCs), and N1 neutrophils), thereby initiating a cascade of tumor cell killing mechanisms, resulting in the efficient presentation of both tumor-associated and neoantigens, and the generation of a functionally active adaptive antitumor immunity via tumor antigen-specific $CD4^+$ and $CD8^+$ effector and memory T cells.[6,9,10]

Toward clinical translation, we have focused on optimizing a lead candidate. The rationale was to develop a therapy candidate that is noninfectious toward plants to avoid any limitations of use due to potential plant infectivity. For the initial mouse work and treatment of canine patients, virus-like particles of CPMV were used. These virus-like particles are termed empty CPMV (eCPMV) because these formulations are devoid of RNA.[11] Potent efficacy was demonstrated in mouse models[6] and canine patients.[12] Nevertheless, when compared to native RNA-laden CPMV, native CPMV outperforms eCPMV in terms of immune activation and antitumor efficacy.[3,13] This differential efficacy is explained by the lack of RNA in eCPMV and hence the lack of engagement of TLR7 signaling,[10] which is stimulated by the single-strand RNA like the viral genome, while TLR2 and 4 are engaged by the capsid proteins. With CPMV, TLR7 signaling uniquely generates the secretion of type-I interferons, which potentiate the antitumor immunotherapy induced

by intratumoral CPMV. In our previous studies, we also developed inactivated CPMV formulations; these contain RNA but are rendered noninfectious by the use of chemical or UV-induced crosslinking.[14,15] In one study, we analyzed UV-inactivated CPMV and found that UV doses needed to inactivate CPMV and render it noninfectious to plants (7.5 J cm^{-2}) and heavily cross-linked the RNA rendering it inaccessible to TLR7 signaling.[14] In a different study, chemically inactivated CPMV was studied and 50 mM of beta-propiolactone or 1 mM of formalin exposure was determined to be sufficient to inactivate CPMV and prevented plant infection.[15] However, again inactivated CPMV had less efficacy compared to its native CPMV counterpart.

Previously, no direct comparisons between CPMV vs UV vs chemically inactivated CPMV were performed, nor did we systematically analyze whether and to what degree TLRs are engaged. This study addresses these information gaps. While we already established that CPMV is the most potent formulation, an inactivated CPMV with greater potency compared to eCPMV but being noninfectious toward plants may be of value—in particular, for the treatment of canine patients where there may be a higher risk of viral shedding in stool or urine. If infectious, CPMV is shed from (canine) patients that could potentially lead to plant infection. While there is currently no evidence that infectious CPMV particles are shed from animal models or humans after ingestion,[16] there are reports that plant viral shedding is detectable in human feces.[17] CPMV infects black-eyed peas and other crops that are grown in the United States. Therefore, with agronomical safety in mind, we here further elaborate on the efficacy and mechanism of action of CPMV vs inactivated CPMV treated with UV light or formalin.

EXPERIMENTAL SECTION

CPMV Production and UV and Formalin Inactivation.

CPMV was propagated in and purified from *Vigna unguiculata* plants, as previously described.[18] UV and formalin inactivation was carried out using previously established methods;[15] in brief, native CPMV (1 mg mL^{-1}) was exposed to UV light at a wavelength of 254 nm using a dose of 7.5 J cm^{-2} from a UVP cross-linker (Analytik Jena AG). For formalin activation, CPMV was treated with 1 mM formalin (Electron Microscopy Sciences) for 5 days at 37 °C. Formalin was then removed by ultrapelleting CPMV at 112,000 g for 1 h at 4 °C. CPMV was stored and handled in a 0.1 M potassium phosphate buffer, and buffer was exchanged to phosphate-buffered saline (PBS) (pH 7.2) for animal studies. A dose of 7.5 J cm^{-2} UV light or 1 mM formalin renders CPMV noninfectious, which was confirmed as outlined in ref 15.

Characterization of Native CPMV and Inactivated CPMV: UV-CPMV and Form-CPMV.

UV/Vis Spectroscopy.—The concentration of native CPMV (CPMV), UV-, and Form-CPMV was determined by UV/vis spectroscopy using a NanoDrop Spectrophotometer (Thermo Fisher Scientific) and the Beer−Lambert law. CPMV: ε (260 nm) = 8.1 mL mg^{-1} cm^{-1}, molecular weight of CPMV = 5.6×10^6 g mol^{-1}.

Gel Electrophoresis.—CPMV, UV-, and Form-CPMV (10 μg) were mixed with a 4 × LDS loading dye (Thermo Fisher Scientific) and denatured (100 °C for 5 min). Samples were then analyzed on 4−12% sodium dodecyl sulfate poly(acrylamide) gel electrophoresis (SDS-PAGE) precast gels in a 1 × morpholinepropanesulfonic acid (MOPS) buffer (Thermo Fisher Scientific). SeeBlue Plus2 ladder (Thermo Fisher Scientific) was used, and gels were run for 35 min at 200 V and 120 mA. Gels were stained with either GelRed (Biotium) or Coomassie Brilliant Blue G-250 (0.25% w/v) and subsequently imaged with the FluorChem R imaging system under UV light or white light. ImageJ software (https://imagej.nih.gov/ij/download.html) and band analysis tool were used for image analysis.

Native CPMV, UV-, and Form-CPMV (10 μg) were analyzed on agarose gels (0.8% w/v) in 1 × tris-acetate-ETDA (TAE) running buffer in the presence of nucleic acid gel stain (GelRed, Biotium). Gels were run for 30 min at 120 V and then imaged under UV light. Alternatively, gels were stained with Coomassie Brilliant Blue G-250 (0.25% w/v, Sigma-Aldrich) and subsequently imaged under white light. A FluorChem R imaging system (Protein Simple) was used.

Transmission Electron Microscopy (TEM).—Formvar copper grids coated with carbon film (Electron Microscopy Sciences) were treated using a PELCO easiGlow operating system to render the grids more hydrophilic. CPMV, UV-, and Form-CPMV (10 μL of drops of sample at 0.5 μg μg^{-1}) were applied onto the grids. After 2 min at room temperature, the grids were washed twice with deionized water for 30 s and then stained twice with 2% (w/v) uranyl acetate (Agar Scientific) for 45 s. A Tecnai transmission electron microscope was used to capture images of the samples at 80 kV.

Dynamic Light Scattering (DLS).—CPMV preparations were analyzed at 1 mg mL^{-1} using a Zetasizer Nano ZSP/Zen5600 instrument (Malvern Panalytical). The particle diameter was calculated as the weighted mean of the intensity distribution.

Size Exclusion Chromatography (SEC).—CPMV, UV-, and Form-CPMV (200 μL (1 mg mL^{-1})) were analyzed using a Superose 6 Increase column and an ÄKTA Explorer chromatography system (GE Healthcare). The flow rate was set to 0.5 mL min^{-1} in a 0.1 M potassium phosphate buffer (pH 7.0), and the absorbance at 260 and 280 nm was recorded.

CPMV In Situ Vaccination.

All tumor treatment experiments were conducted in accordance with the University of California, San Diego Institutional Animal Care and Use Committee and involved female C57BL/6 mice (The Jackson Laboratory) 6−8 weeks of age.

A dermal melanoma tumor model was established by the intradermal injection of 2.0×10^5 B16F10 cells in 30 mL of PBS into the skin of the right flank of C57BL/6 mice on day 0. CPMV, UV-CPMV, and Form-CPMV (100 μg) were administered by intratumoral injection in 20 μL of PBS; weekly treatment was given starting ~9 days post tumor challenge when tumors reached ~60 mm^3. Tumor volumes were measured using a digital caliper. The tumor volume (mm^3) was calculated as follows: V = (L x W x W)/2, where V is tumor volume,

W is tumor width, L is tumor length. Animals were euthanized when the tumor volume exceeded 1500 mm^3.

All results are expressed as the mean ± standard error of the means (SEM), as indicated. Student's *t*-test was used to compare the statistical difference between two groups, and one-way or two-way analysis of variance (ANOVA) with Sidak's or Tukey's multiple comparison tests was used to compare three or more groups. Survival rates were analyzed using the log-rank (Mantel−Cox). *P*-values < 0.05 were considered statistically significant: (*$p < 0.05$, **$p < 0.05$, etc.). All statistical tests were performed using GraphPad Prism v7.0 (GraphPad Software).

Immunological Assays.

Animals.—Female C57BL/6 mice (6−8 weeks old) were purchased from The Jackson Laboratory. $TLR7^{-/-}$ were originally purchased from The Jackson Laboratory and genotyped and bred at Dartmouth College. All mouse studies were approved by the Institutional Animal Care and Use Committee of Dartmouth College.

Cell Culture and Cytokine Quantification.—B16F10 melanoma cells were grown in Dulbecco's modified Eagle's medium (DMEM) supplemented with 10% (v/v) fetal bovine serum (FBS) and 1% (v/v) penicillin−streptomycin. Spleens from C57BL/6 mice or $TLR7^{-/-}$ mice were harvested, and 5×10^5 splenocytes were cultured with either CPMV or UV- or Form-CPMV (12 μg/mL) in 200 μL of complete RPMI for 24 h in 96-well plates. The conditioned medium was stored frozen (−20 °C) prior to assay by enzyme-linked immunosorbent assay (ELISA) to detect interleukin-6 (IL-6) or interferon α (IFN-α), as previously described.[10] Unless otherwise noted, these cells were cultured in RPMI1640 supplemented with 10% v/v FBS and antibiotics. All cell cultures were maintained in a 5% CO_2 incubator at 37 °C.

Statistics.—Data are presented as the average means ± standard error of the means (SEM). The results shown here are representative responses from multiple experiments, which are repeated at least once with similar results. *T*-test *p*-values < 0.05 were required to assign significance and are represented as an asterisk (*) in the figures and $p < 0.01$ as ** and $p < 0.001$ as ***.

RESULTS AND DISCUSSION

Synthesis and Characterization of CPMV, UV-CPMV, and Form-CPMV.

CPMV, UV-CPMV, and Form-CPMV preparations were analyzed by gel electrophoresis (denaturing SDS-PAGE and native agarose gel electrophoresis) as well as size exclusion chromatography (SEC) and transmission electron microscopy (TEM). SDS-PAGE separates the genomic RNA and coat proteins (Figure 1A,B). Intact CPMV particles form 30 nm sized icosahedrons with a pseudo = 3 symmetry.[18] CPMV has a bipartite +sense ssRNA genome with RNA-1 (6 kb) and RNA-2 (3.5 kb) encapsidated separately into identical particles composed of 60 copies each of a small (*S*, 24 kDa) and large (*L*, 42 kDa) coat protein. The *S* and *L* proteins are separated on SDS-PAGE with no apparent differences between

the CPMV, UV-, and Form-CPMV preparations. Clear differences are detected on the RNA level. SDS-PAGE does not resolve the length differences between RNA-1 vs RNA-2; we can only detect the total genomic RNA. Aggregation of the viral RNA is apparent for both the UV- and formalin-inactivated CPMV preparations. This is as expected because these viral inactivation methods create RNA−RNA and RNA−protein cross-links, therefore preventing translation and replication. When comparing the UV- vs Form-CPMV, a higher degree of RNA aggregation is induced by UV treatment (Figure 1A).

This is consistent with findings from native agarose gel electrophoresis where intact CPMV is analyzed. It is noted that the RNA signals increase upon UV or formalin treatment with greater fluorescence observed (from the GelRed nucleic acid staining) for UV-CPMV > Form-CPMV > native CPMV (Figure 1C,D). This suggests that more cross-links are induced during UV inactivation, therefore allowing the more secondary structure to occur that would lead to a higher degree of GelRed dye intercalation. It is also noted that UV-treated CPMV preparations contain free RNA, which may indicate particle breakage and leakage (Figure 1C). The protein staining indicates the presence of intact CPMV, some aggregated Form-CPMV, and more heavily aggregated UV-CPMV (Figure 1D); this is consistent with UV and formalin inducing not only RNA−RNA cross-links but also RNA−protein cross-links—formalin may also introduce protein−protein cross-links.[19]

TEM imaging shows intact CPMV; the Form-CPMV preparations also appear intact with no detectable particle breakage but some interparticle aggregation (Figure 1E). It is noted that the UAc negative stain stains the formalin-treated CPMV more intensely compared to untreated CPMV. Lastly, the UV-CPMV mostly appeared intact; however, some aggregation is apparent and broken particles are also visible (Figure 1E), which explains the partial loss of RNA observed in Figure 1D.

DLS measured CPMV at 39.5 nm, Form-CPMV at 48.5 nm, and UV-CPMV at 74.3 nm (Figure 1F), which is in agreement with all other characterization methods and indicates that UV-CPMV is more heavily aggregated than Form-CPMV. This was further corroborated by SEC analysis. SEC analysis using a Superose 6 Increase column and an ÄKTA Explorer showed intact CPMV and Form-CPMV, which is consistent with TEM. CPMV and Form-CPMV elute at ~14 mL from the column with an A260/A280 absorbance ratio of ~1.8, which is in agreement with intact particle preparations (Figure 1G). The elution profile for UV-CPMV was more complex, showing a mix of aggregated CPMV, intact CPMV, and broken particles—particles that elute at 14 mL show a slightly lower A260/A280 absorbance ratio of ~1.7, which is indicative of RNA loss. Overall, these data are in good agreement with the properties of Form- and UV-CPMV formulations prepared by us previously.[14,15]

Efficacy and Mechanism of Action of CPMV, UV-, and Form-CPMV In Situ Vaccination against Melanoma.

To investigate the therapeutic efficacy of CPMV, UV-, and Form-inactivated CPMV against solid tumors, we established a mouse melanoma model by intradermal transplantation of B16F10 cells. B16F10 melanoma-bearing mice received weekly intratumoral treatment using CPMV, UV-CPMV, and Form-CPMV vs PBS; treatment began on day 9 post tumor challenge when tumor volumes reached ~60 mm^3 (Figure 2A). As expected, CPMV

treatment demonstrated potent efficacy with significant tumor growth inhibition compared to the PBS-treated group ($P < 0.05$; Figure 2B,C). The mean tumor volume administered with CPMV was <100 mm^3 on day 23, the last day of dosing. Inactivation of CPMV attenuated its efficacy but to different degrees, with UV-CPMV being the least efficacious—tumors measured 500 mm^3 on day 23; in stark contrast, the Form-CPMV showed more potent efficacy, with tumors averaging 140 mm^3 on day 23, albeit still larger on average than CPMV-treated tumors (although not a statistically significant difference). Both CPMV and Form-CPMV generated a statically significant improvement in survival compared to PBS, but there was no significant difference between UV-CPMV and PBS (CPMV vs UV-CPMV; $p = 0.0034$**, CPMV vs Form-CPMV; $p = 0.0783$ n.s., CPMV vs PBS; $p = 0.0003$***, Form-CPMV vs PBS; $p = 0.0297$*, UV-CPMV vs PBS; 0.2150 n.s.; Figure 2D). Overall, the median survival time for the group of CPMV was undefined because the survival rate was greater than 50%, with an 87% survival at the day 40 experimental endpoint. Form-CPMV, UV-CPMV, and PBS control groups exhibited mean survival times of 36, 27, and 26 days, respectively. Together, the efficacy study demonstrates the potent efficacy of CPMV and Form-CPMV—however, UV-CPMV as prepared here did not reduce tumor growth rate or improve survival.

Next, to assess immune cell responses to each reagent, we analyzed cytokine stimulation from splenocyte cocultures using C57BL/6 mice and $TLR7^{-/-}$ mice. Splenocytes were isolated and incubated with CPMV, Form-CPMV, and UV-CPMV and then analyzed by ELISA to detect either IL-6 or IFN-α. Overall data indicate that formalin inactivation preserves most of CPMV's immunogenic properties (Figure 3). Form-CPMV induced comparable levels of IL-6 when compared to native CPMV; in stark contrast, UV-CPMV induced less IL-6 yet still generated significantly increased levels of IL-6 as compared to PBS (Figure 3). A similar trend was observed when splenocytes from $TLR7^{-/-}$ mice were used; there was no increase of IL-6 compared to PBS-treated splenocytes from UV-CPMV, but Form-CPMV and CPMV induced significant IL-6 albeit at lower levels compared to splenocytes isolated from the wild-type mice of strain C57BL/6. This makes sense since proinflammatory cytokines and chemokines are among the end products of the TLR7 signaling pathway.[10] UV-CPMV induction of much less IL-6 in normal mice agrees with our previous findings.[14]

Type-I interferons are key signatures of TLR7 signaling; therefore, we analyzed IFN-α secretion. CPMV signals through TLR7 and induces IFN-α secretion in wild-type mice, which is lost in $TLR7^{-/-}$ knockout mice and confirms our previous data.[10] We also previously found that UV-CPMV is a poor TLR7 stimulant and hence does not induce significant levels of type-I IFNs (Figure 3) and this is in agreement with previous findings.[14] Interestingly, Form-CPMV induces significant levels of IFN-α albeit slightly less than CPMV; the ratio of IFN-α between native CPMV and Form-CPMV is 1.3 and is statistically significant. Given that RNA is cross-linked as evident from SDS-PAGE and native gel electrophoresis (Figure 1A–E), it is fair to conclude that the RNA may become less accessible to activate TLR7 since differences in cell uptake comparing native and inactivated CPMV were not apparent.[15] For the UV-CPMV samples, limited efficacy was observed (Figure 2). We note key differences in the nanoparticle characteristics: data indicate that UV-CPMV is more extensively cross-linked including RNA and protein cross-links as well

as interparticle cross-links that result in aggregation. Some broken particles and partial loss of RNA were also evident. Therefore, a multitude of factors may explain the lack of TLR7 signaling and reduced efficacy: UV treatment may lead to partial denaturation of the proteins, which may render their immunogenicity; the larger aggregates likely have altered cell uptake and trafficking properties compared to well-dispersed CPMV and Form-CPMV, and finally broken particles and RNA loss will reduce TLR7 interactions. All of these may be the underlying factors that contribute to the differential efficacy that was observed.

Our data highlight the potency of CPMV as well as its inactivated counterpart Form-CPMV for cancer immunotherapy. In particular, the inactivated version (Form-CPMV) may be a suitable lead candidate for translation into the clinic because Form-CPMV confers efficacy while maintaining agronomical safety; i.e., the Form-CPMV nanoparticles are noninfectious toward plants.[15]

CPMV has unique potency and it outperforms classical adjuvants[6] as well as other plant viruses.[3] CPMV is more potent compared to small-molecule TLR or STING agonists.[6,10] This can be explained by the nanoparticle character enabling prolonged tumor retention and multivalent and multipronged engagement of TLR receptors.[6,20] Hence, CPMV offers advantages compared to synthetic small-molecule therapeutics because it mimics a viral pathogen or danger signal more closely. Additional advantages are conferred over mammalian oncolytic therapies: production through plant molecular farming is highly scalable and high yielding; 1 mg of CPMV can be obtained per 1 g of infected leaf tissue. Plant viruses are stable and do not require cold-chain storage;[21] in contrast, oncolytic immunotherapy T-VEC must be stored in ultralow freezers. Plant viruses may be safer than mammalian viruses because they do not infect mammals. It is also important to note that CPMV-ISV is conceptually distinct from oncolytic cancer therapy: oncolytic viruses function by targeting and killing cancer—however, CPMV targets innate immune cells to prime systemic anti-immunity (adaptive arm). Because CPMV targets the innate immune system, the presence of carrier-specific antibodies is not neutralizing: anti-CPMV antibodies opsonize CPMV and enable faster update in innate cells—the target cell type—and therefore enhance (rather than neutralize) CPMV efficacy after repeated administration.[22] Altogether, CPMV and its inactivated counterpart, Form-CPMV, provide intriguing candidate nanotechnology for cancer immunotherapy.

CONCLUSIONS

These data provide critical insights into the optimal approach to inactivate CPMV while maintaining efficacy as in situ vaccine in the context of cancer immunotherapy (Scheme 1). While both methods of inactivation result in noninfectious CPMV, the UV inactivation modifies the CPMV particles more extensively and therefore abolishes TLR7 signaling. In contrast, Form-CPMV preserves the structural and biological properties of CPMV. Formalin treatment also leads to RNA and protein cross-links, which explain the slightly reduced type-I IFN generation by RNA-induced TLR7 signaling. Nevertheless, Form-CPMV maintained antitumor efficacy compared to CPMV. Form-CPMV had much better antitumor efficacy compared to UV-CPMV, and in these studies, they did not statistically differ from CPMV in that regard, despite subtle indications of less efficacy. The data clearly

show that for further efforts to develop, an inactivated CPMV reagent for future clinical use could focus on Form-CPMV.

More mechanistic studies may include studying the intratumoral as well as intracellular trafficking of inactivated vs native CPMV. As outlined in the Results and Discussion section, a multitude of factors may contribute to the loss of TLR7 signaling for UV-CPMV but not Form-CPMV; this may include the cross-linked state of the RNA as well as the degree of RNA−protein cross-links, but also intratumoral distribution and cellular uptake and trafficking likely impact the fate of the inactivated vs native CPMV formulations. Beyond formalin and UV treatment, alternative inactivation methods such as treatment with heat, chaotropic salts, detergents, gamma irradiation, hydrogen peroxide, etc., may also be considered.[23] Of course, one may think of additional pathways to generate noninfectious, yet RNA-laden CPMV. In one approach, one may separate the RNA-1- vs RNA-2-containing particles (referred to as the bottom and middle components of CPMV)[24] or in another approach one could consider developing an expression system that leads to CPMV packaging designer RNAs[25] as opposed to its genome. Therefore, if determined that a noninfectious CPMV formulation is needed for clinical translation, there are a multitude of approaches toward achieving this goal.

Funding

This work was funded, in part, through the following NIH grants R01 CA253615, R01 CA274640, and R01 CA224605 and CDMRP award W81XWH2010742 (to N.F.S.) as well as training grant T32EB005970 (to E.C.K.).

REFERENCES

(1). (a)Lemke-Miltner CD; Blackwell SE; Yin C; Krug AE; Morris AJ; Krieg AM; Weiner GJ Antibody Opsonization of a TLR9 Agonist-Containing Virus-like Particle Enhances In Situ Immunization. J. Immunol 2020, 204, 1386–1394. [PubMed: 31953355] (b)Cheng N; Watkins-Schulz R; Junkins RD; David CN; Johnson BM; Montgomery SA; Peine KJ; Darr DB; Yuan H; McKinnon KP; et al. A nanoparticle-incorporated STING activator enhances antitumor immunity in PD-L1-insensitive models of triple-negative breast cancer. JCI Insight 2018, 3, No. e120638. (c)Brody JD; Ai WZ; Czerwinski DK; Torchia JA; Levy M; Advani RH; Kim YH; Hoppe RT; Knox SJ; Shin LK; et al. In situ vaccination with a TLR9 agonist induces systemic lymphoma regression: a phase I/II study. J. Clin. Oncol 2010, 28, 4324–4332. [PubMed: 20697067]

(2). Ferrucci PF; Pala L; Conforti F; Cocorocchio E. Talimogene Laherparepvec (T-VEC): An Intralesional Cancer Immunotherapy for Advanced Melanoma. Cancers 2021, 13, No. 1383.

(3). Shukla S; Wang C; Beiss V; Cai H; Washington T 2nd; Murray AA; Gong X; Zhao Z; Masarapu H; Zlotnick A; et al. The unique potency of Cowpea mosaic virus (CPMV) in situ cancer vaccine. Biomater. Sci 2020, 8, 5489–5503. [PubMed: 32914796]

(4). Lebel ME; Chartrand K; Tarrab E; Savard P; Leclerc D; Lamarre A. Potentiating Cancer Immunotherapy Using Papaya Mosaic Virus-Derived Nanoparticles. Nano Lett. 2016, 16, 1826–1832. [PubMed: 26891174]

(5). Murray AA; Wang C; Fiering S; Steinmetz NF In Situ Vaccination with Cowpea vs Tobacco Mosaic Virus against Melanoma. Mol. Pharm 2018, 15, 3700–3716. [PubMed: 29798673]

(6). Lizotte PH; Wen AM; Sheen MR; Fields J; Rojanasopondist P; Steinmetz NF; Fiering S. In situ vaccination with cowpea mosaic virus nanoparticles suppresses metastatic cancer. Nat. Nanotechnol 2016, 11, 295–303. [PubMed: 26689376]

(7). (a)Hoopes PJ; Mazur CM; Osterberg B; Song A; Gladstone DJ; Steinmetz NF; Veliz FA; Bursey AA; Wagner RJ; Fiering SN In Effect of Intra-Tumoral Magnetic Nanoparticle Hyperthermia and Viral Nanoparticle Immunogenicity on Primary and Metastatic Cancer, Proc.

SPIE 10066, Energy-based Treatment of Tissue and Assessment IX; SPIE: San Francisco, California, United States, 2017; Vol. 10066.(b)Hoopes PJ; Moodie KL; Petryk AA; Petryk JD; Sechrist S; Gladstone DJ; Steinmetz NF; Veliz FA; Bursey AA; Wagner RJet al. In Hypo-Fractionated Radiation, Magnetic Nanoparticle Hyperthermia and a Viral Immunotherapy Treatment of Spontaneous Canine Cancer, Proc. SPIE 10066, Energy-based Treatment of Tissue and Assessment IX; SPIE, 2017; Vol. 10066.(c)Hoopes PJ; Wagner RJ; Duval K; Kang K; Gladstone DJ; Moodie KL; Crary-Burney M; Ariaspulido H; Veliz FA; Steinmetz NF; Fiering SN Treatment of Canine Oral Melanoma with Nanotechnology-Based Immunotherapy and Radiation. Mol. Pharm 2018, 15, 3717–3722. [PubMed: 29613803]

(8). Kawamura T; Ogawa Y; Aoki R; Shimada S. Innate and intrinsic antiviral immunity in skin. J. Dermatol. Sci 2014, 75, 159–166. [PubMed: 24928148]

(9). Wang C; Fiering S; Steinmetz NF Cowpea Mosaic Virus Promotes Anti-Tumor Activity and Immune Memory in a Mouse Ovarian Tumor Model. Adv. Therapeutics 2019, 2, No. 1900003.

(10). Mao C; Beiss V; Fields J; Steinmetz NF; Fiering S. Cowpea mosaic virus stimulates antitumor immunity through recognition by multiple MYD88-dependent toll-like receptors. Biomaterials 2021, 275, No. 120914.

(11). Saunders K; Sainsbury F; Lomonossoff GP Efficient generation of cowpea mosaicvirus empty virus-like particles by the proteolytic processing of precursors in insect cells and plants. Virology 2009, 393, 329–337. [PubMed: 19733890]

(12). Alonso-Miguel D; Valdivia G; Guerrera D; Perez-Alenza MD; Pantelyushin S; Alonso-Diez A; Beiss V; Fiering S; Steinmetz NF; Suarez-Redondo M; et al. Neoadjuvant in situ vaccination with cowpea mosaic virus as a novel therapy against canine inflammatory mammary cancer. J. Immunother. Cancer 2022, 10, No. e004044.

(13). Wang C; Beiss V; Steinmetz NF Cowpea Mosaic Virus Nanoparticles and Empty Virus-Like Particles Show Distinct but Overlapping Immunostimulatory Properties. J. Virol 2019, 93, No. e00129–19.

(14). Koellhoffer EC; Mao C; Beiss V; Wang L; Fiering SN; Boone CE; Steinmetz NF Inactivated Cowpea Mosaic Virus in Combination with OX40 Agonist Primes Potent Antitumor Immunity in a Bilateral Melanoma Mouse Model. Mol. Pharm 2022, 19, 592–601. [PubMed: 34978197]

(15). Chariou PL; Beiss V; Ma Y; Steinmetz NF In situ vaccine application of inactivated CPMV nanoparticles for cancer immunotherapy. Mater. Adv 2021, 2, 1644–1656. [PubMed: 34368764]

(16). Affonso de Oliveira JF; Chan SK; Omole AO; Agrawal V; Steinmetz NF In Vivo Fate of Cowpea Mosaic Virus In Situ Vaccine: Biodistribution and Clearance ACS Nano 2022, DOI: 10.1021/acsnano.2c06143.

(17). Rosario K; Symonds EM; Sinigalliano C; Stewart J; Breitbart M. Pepper mild mottle virus as an indicator of fecal pollution. Appl. Environ. Microbiol 2009, 75, 7261–7267. [PubMed: 19767474]

(18). Murray AA; Sheen MR; Veliz FA; Fiering SN; Steinmetz NF In Situ Vaccination of Tumors Using Plant Viral Nanoparticles. Methods Mol. Biol 2019, 2000, 111–124. [PubMed: 31148013]

(19). Wilton T; Dunn G; Eastwood D; Minor PD; Martin J. Effect of formaldehyde inactivation on poliovirus. J. Virol 2014, 88, 11955–11964. [PubMed: 25100844]

(20). Stump CT; Ho G; Mao C; Veliz FA; Beiss V; Fields J; Steinmetz NF; Fiering S. Remission-Stage Ovarian Cancer Cell Vaccine with Cowpea Mosaic Virus Adjuvant Prevents Tumor Growth. Cancers 2021, 13, No. 627.

(21). Chung YH; Church D; Koellhoffer EC; Osota E; Shukla S; Rybicki EP; Pokorski JK; Steinmetz NF Integrating plant molecular farming and materials research for next-generation vaccines. Nat. Rev. Mater 2022, 7, 372–388. [PubMed: 34900343]

(22). Shukla S; Wang C; Beiss V; Steinmetz NF Antibody Response against Cowpea Mosaic Viral Nanoparticles Improves In Situ Vaccine Efficacy in Ovarian Cancer. ACS Nano 2020, 14, 2994–3003. [PubMed: 32133838]

(23). Elveborg S; Monteil VM; Mirazimi A. Methods of Inactivation of Highly Pathogenic Viruses for Molecular, Serology or Vaccine Development Purposes. Pathogens 2022, 11, No. 271.

(24). Steinmetz NF; Evans DJ; Lomonossoff GP Chemical introduction of reactive thiols into a viral nanoscaffold: a method that avoids virus aggregation. ChemBioChem 2007, 8, 1131–1136. [PubMed: 17526061]

(25). Peyret H; Lomonossoff GP Specific Packaging of Custom RNA Molecules into Cowpea Mosaic Virus-like Particles. Methods Mol. Biol 2022, 2480, 103–111. [PubMed: 35616860]

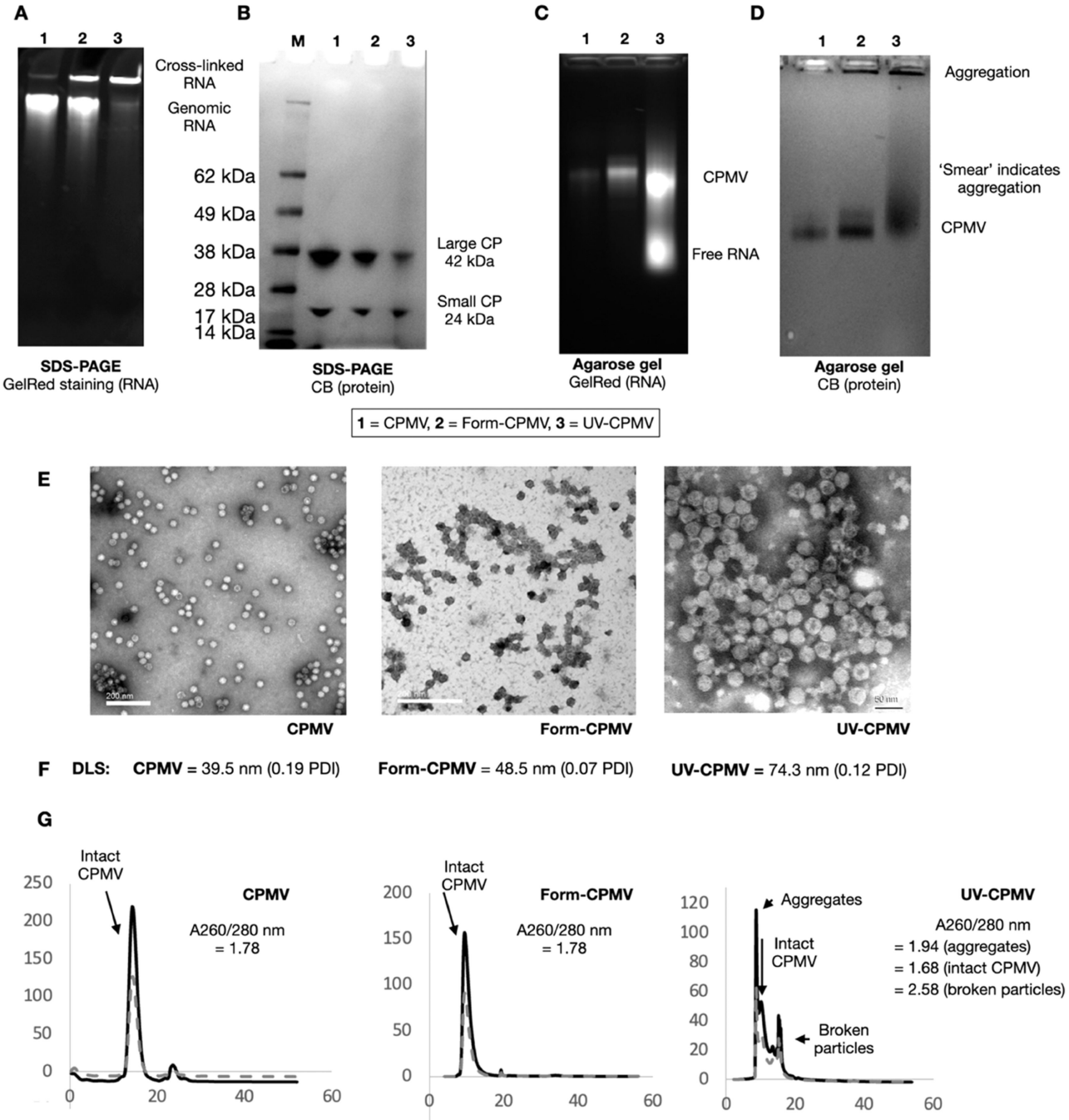

Figure 1.

Characterization of CPMV, Form-CPMV, and UV-CPMV. (A, B) SDS-PAGE stained with GelRed and imaged under UV light or stained with Coomassie blue (CB) and imaged under white light. (C, D) Native agarose gel electrophoresis stained with GelRed and imaged under UV light or stained with Coomassie blue (CB) and imaged under white light. (E) TEM imaging of negatively stained CPMV, Form-CPMV, and UV-CPMV. The scale bar is 200 nm for CPMV and Form-CPMV and 50 nm for UV-CPMV. (F) Hydrodynamic radius

and polydispersity index (PDI) of CPMV preparations as determined by DLS. (G) SEC of CPMV, Form-CPMV, and UV-CPMV.

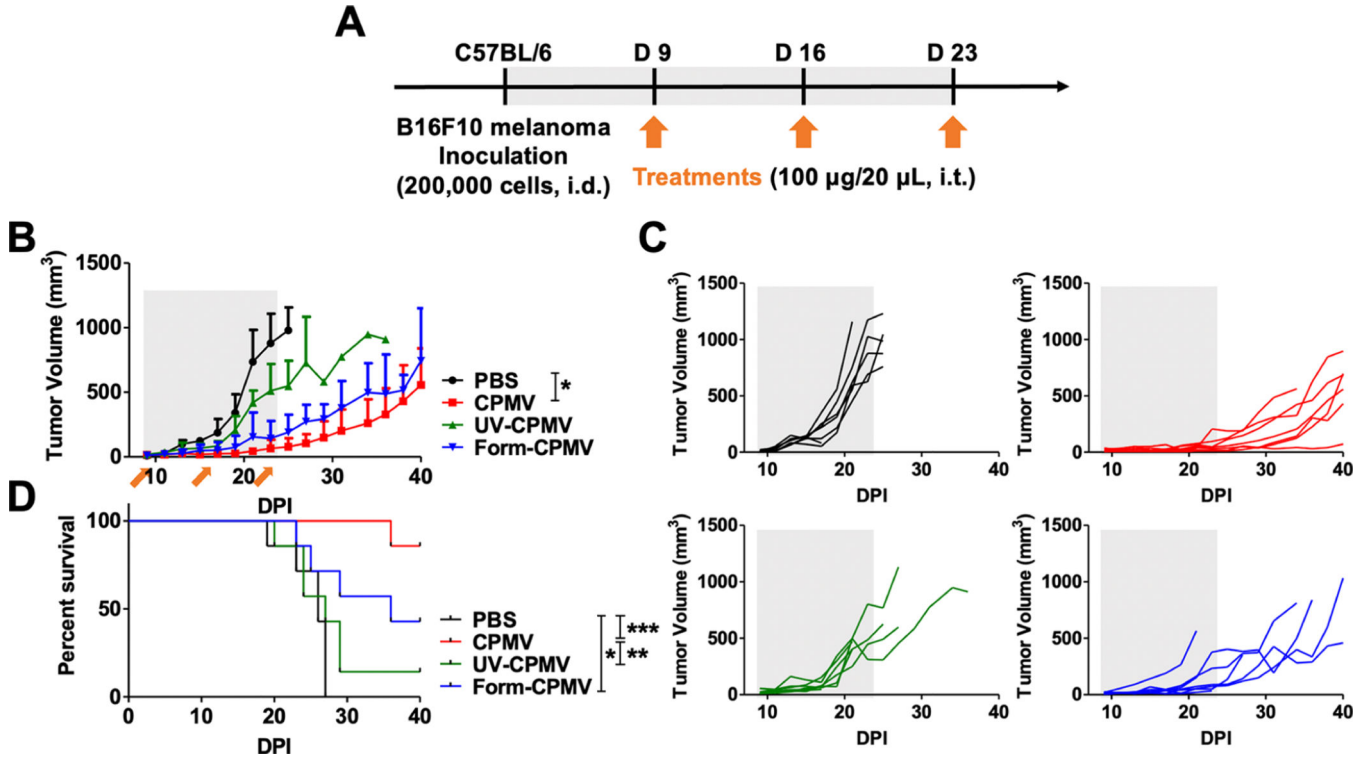

Figure 2.

In vivo therapeutic efficacy of CPMV, Form-CPMV, and UV-CPMV. (A) Schematic representation of the experimental timeline for the B16F10 melanoma model. C57BL/6 mice were intradermally (i.d.) injected with 200,000 B16F10 melanoma cells. CPMV, Form-CPMV, and UV-CPMV (100 μg/20 μL in PBS) were administrated intratumorally (i.t.) on days 9, 16, and 23 postinoculation of B16F10 melanoma cells. (B) Tumor growth curves of mice bearing B16F10 after treatments of CPMV, Form-CPMV, and UV-CPMV three times. Orange arrows indicate treatment time points. Results were compared using an unpaired *t*-test (*$p < 0.05$). Data are means ± SEM ($n = 7$). (C) Individual tumor growth curves in each treatment group (black; PBS, red; CPMV, green; UV-CPMV, and blue; Form-CPMV). Gray shaded boxes indicate the treatment period. (D) Survival curves of mice after treatments. Results were analyzed by log-rank (Mantel−Cox) test (*$p < 0.05$, **$p < 0.01$, ***$p < 0.001$).

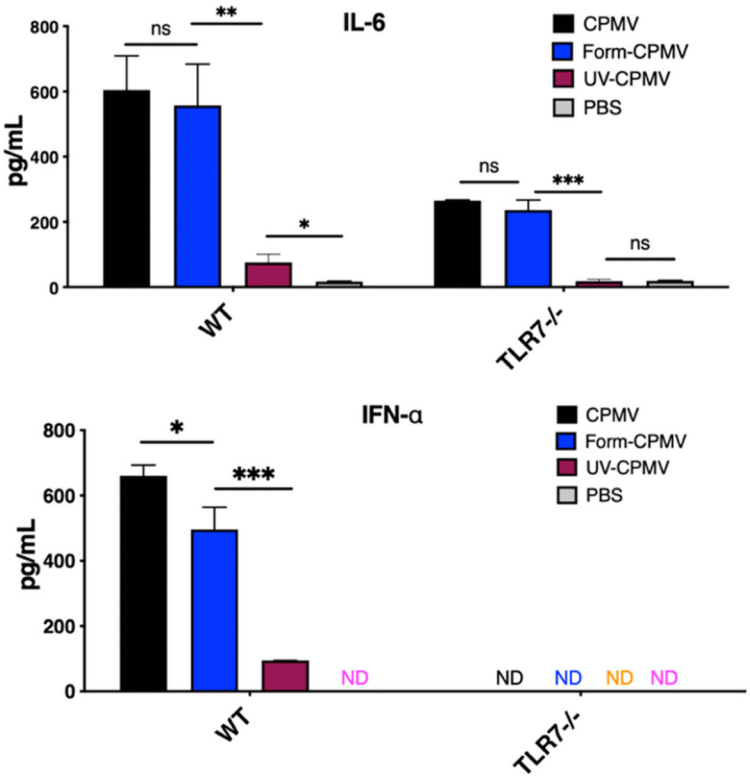

Figure 3.

Formalin inactivation retains the majority of CPMV immunogenicity. Splenocytes of the corresponding mouse strain were cultured for 24 h with CPMV, formalin-inactivated CPMV, or UV-inactivated CPMV, and cytokine levels were analyzed by IL-6 (upper panel) or IFN-α (lower panel) ELISAs ($n = 3$). Data for bar graphs calculated using unpaired Student's t-test with $p > 0.05$ as ns, $p < 0.05$ as *, $p < 0.01$ as **, and $p < 0.001$ as ***.

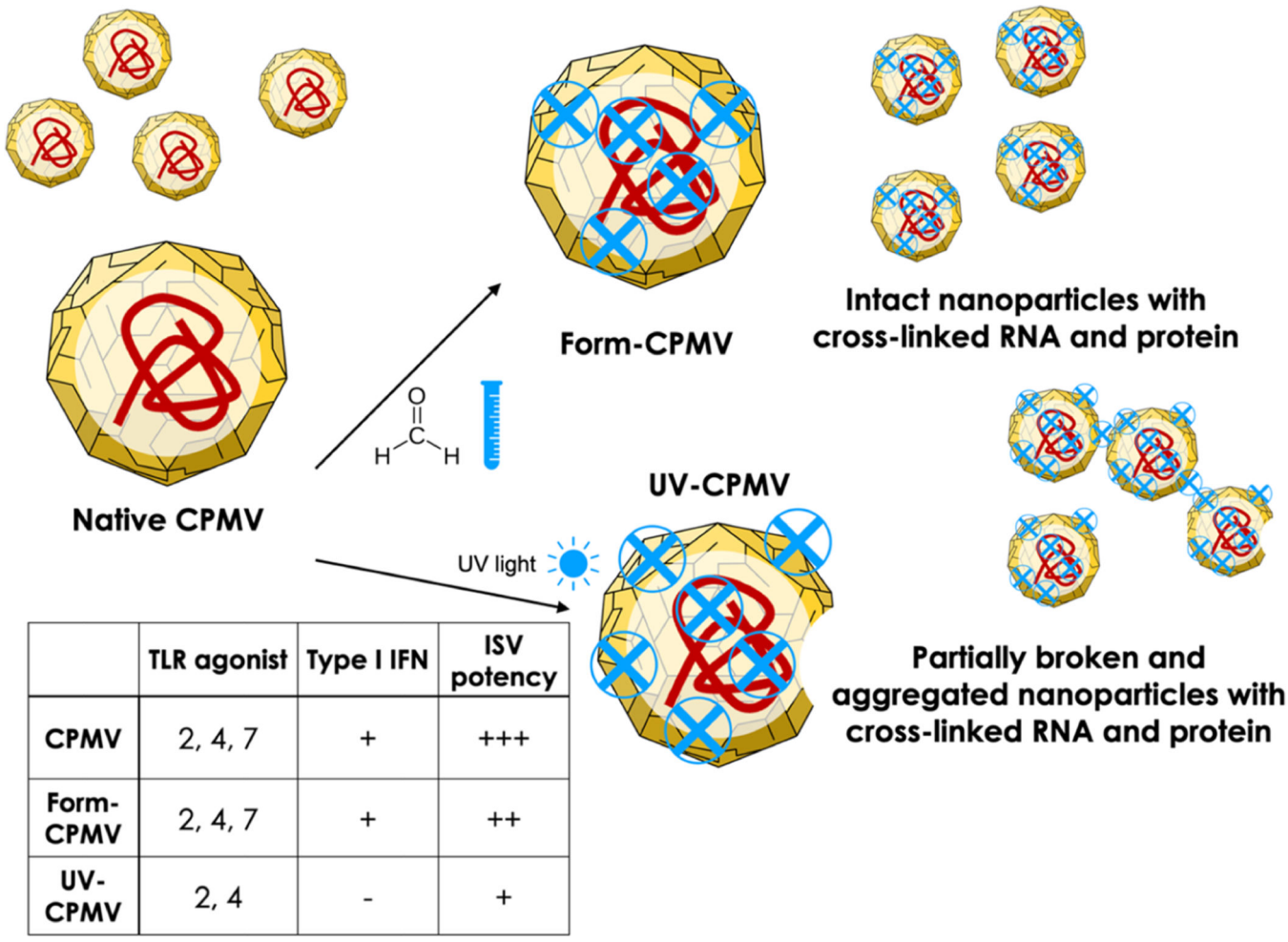

	TLR agonist	Type I IFN	ISV potency
CPMV	2, 4, 7	+	+++
Form-CPMV	2, 4, 7	+	++
UV-CPMV	2, 4	-	+

Scheme 1.

CPMV Structure Showing the Protein Capsid (in Yellow) and RNA (in Red)[a]

[a] Treatment with formaldehyde results in RNA/protein cross-linking but maintains intact and dispersed Form-CPMV nanoparticles, which signal through TLR2, 4, and 7 generating type-I interferon responses and antitumor efficacy when applied as ISV, albeit at lower efficacy compared to native CPMV. UV-cross-linking of CPMV results in the cross-linking of RNA and protein as well as interparticle cross-linking (aggregation) and partially broken particles; UV-CPMV does not signal through TLR7, does not generate type-I interferon, and has limited efficacy as ISV.